Effect of Preheat Variables on Mechanical Properties Weld Zone Dissimilar joint of the MO40 to St-37 by GMAW/GTAW

M. R. Tavighi[1,*], A. Asaadi Zahrai[2], M. Ghanbari Haghighi[1], B. Karbakhsh Ravari[1]

[1]*Advanced Materials Engineering Research Center, Karaj Branch, Islamic Azad University, Karaj Iran.*
[2]*Faculty of Materials Science and Engineering Khajeh Nasir Toosi University, Tehran.Iran.*
Received: 26 October 2021 - Accepted: 15 February 2022

Abstract

Joining of dissimilar metals is one of the most important requirements of different industries. The joining of alloy and plain carbon steels is typically involved in the manufacturing process, and this is because in this case, the cost required for the raw materials is reduced. On the other hand, in the joining of dissimilar metals and alloys, due to their different chemical composition, the strength and quality of the joining joint is largely dependent on the parameters involved in the process. Steel grades 1.7225 (MO40) and St-37 are used in various industries. Due to the conditions, the bond strength of the above steel grades is very important. Therefore, the aim of this study was to investigate the effect of preheating time and temperature parameters on the mechanical properties of the bond formed between the alloy (MO40) 1.7225 and St-37 steel. Studies have shown that among the various parameters, duration and preheating temperature are of great importance in increasing the service life of these parts in the welded state, but so far no detailed study on the duration and The proper preheating temperature for the welding process of steels (MO40) 1.7225 and St-37 is not provided and usually the operating efficiency of these parts is low in severe stress conditions and these parts fail in the welded place.

Keywords: Dissimilar Metals, HAZ, MO40, St37, Preheating.

1. Introduction

In order to achieve the desired properties in the construction of engineering structures, metal alloys with different properties are used together. For this reason, it is necessary to use several metals together, the collection of which provides the required design properties, one of which is the connection of dissimilar metals in different industries[1] .On the other hand, in the joining of dissimilar metals and alloys, due to their different chemical composition, the strength and quality of the joining joint is largely dependent on the variables involved in the process [1,2]. One method of welding is shielded arc welding, which uses carbon dioxide shielding gas called CO_2 welding. Since CO_2 is an active gas, this type of welding falls into the MAG category [3, 4]. It is worth mentioning that CO_2 welding has been introduced as the best method for welding thin and semi-thick non-rigid steel plates, which has grown significantly today in various industries, especially in the field of machinery [5]. One of the most important raw materials that is widely used in various industries is called St37 with reference standard AISI 1015/ DIN 17100 steel. This type of steel is in the range of mild carbon steel and has a certain yield strength 360 MPa.

[*]*Corresponding author*
Email address: taavighi.Mreza@gmail.com

St37 steel is commonly used in the manufacture of building profiles and the construction industry [4].
St37 steel has a very good weldability due to the presence of low carbon in the structure of this steel and this factor has caused this steel to surpass its competitors in this field. St37 steel also has very high mechanical properties, which is the property of St37 steel, has increased the useful life of manufactured products. Steel 1.7225 (Mo40), known as MO40, is one of the most famous and widely used alloy steels for making parts with medium and relatively large cross-section in various industries such as automotive and machinery such as crankshafts, connecting rods, intermediate gears, spindles and rollers of the steel industry. , Resistant screws are used [4, 7].
Welding of 4140 steel is a bit difficult because it is more sensitive to cracking and therefore requires a suitable preheater [8]. In 2015, Aziziyeh et al. [9] conducted research on the welding of St37 and CK60 steels.[10] The results of the tensile test show that the strength of the weld zone is between the strength of the two primary steels. Studies by Serivastava et al. [11] During the welding process, steel is heated, as a result of which the heated part has a different microstructure from the base metal microstructure, which is called the heat-affected region [12, 13].
Jenlang et al. [14- 16] investigated the effect of preheating temperature on the microstructure and joining properties of 42CrMo4 / 38MnVS6 alloy.

42CrMo4 and 38MnVS6 steels are among the medium and low alloy carbon steels. 42CrMo4 steel belongs to Cr-Mo alloy system and has good strength and toughness. The molybdenum element in this steel reduces the brittleness of the steel temperament and increases the high temperature strength.
38MnVS6 belongs to the Mn-V alloy system and vanadium in this steel improves the strength, toughness and plasticity of the steel and also increases the stability of high temperature temper.

2. Materials and Methods

Steel grades (MO40) 1.7225 and St37 are used in the manufacture of various industrial parts. Due to the common use of these parts, with ASTM E standard it is necessary to study the weld strength, impact energy and metallurgical properties created from them [17, 18].
In order to perform the designed tests, steel plates made of St37 structural steel and 1.7225 steel were prepared and subjected to quantometer analysis test with ASTM E 415-08 standard to be sure. In this study, in order to determine the exact chemical composition of the alloys used, the relevant analysis was used according to the reference standard ASTM E 415-17: 2018 and the environmental control standard ASTM E 406-81 (2012): 2018. Table. 1. and Table. 2. show the chemical composition of St37 steel and 1/7225**.**

Table. 1. Chemical composition of St 37steel used in this study (wt.%).

C	Si	Mn	P	S
0.180	0.400	1.600	0.020	0.020

Table. 2. Chemical composition of 1.7225 steel used in this research (wt.%).

C	Si	Mn	P	S	Cr	Ni	Mo
0.420	0.240	0.820	0.020	0.010	1.030	0.250	0.190

In order to investigate the effect of preheating time and temperature variables, 9 modes were considered. The selected preheating temperatures were 250 °C, 350 °C and 450 °C, respectively, and the preheating duration was 10, 15 and 20 minutes, respectively. On the other hand, in order to compare the effect of the above variables on the quality of argon welding, modes 10 to 12 were considered**.**

For welding the desired steel plates, the method of arc welding with CO_2 and TIG shielding gas was used. Based on the test design, the samples were placed for Butt Joint with alloy 1.5125 was used with Ama welding wire filler, 40-18 m diameter .1.2 mm. (DIN 8559: SG 2 or En 440: G3 Si1) welding as Sing V-Groove, in which case the bevel angle of the samples was 17.5 degrees and the Root Face was 2 mm. Table. 3. presents 12 selected modes with sample numbers. Fig. 1. also shows a schematic of how the samples are arranged relative to each other.

Table. 3. Conditions of the samples studied in this study.

Preheating Time (min)	Preheating Temperature (°C)	Sample Number
CO_2 Welding (Mag)		
10	250	**1**
15	250	**2**
20	250	**3**
10	350	**4**
15	350	**5**
20	350	**6**
10	450	**7**
15	450	**8**
20	450	**9**
Argon Welding (TIG)		
10	350	**10**
15	350	**11**
20	350	**12**

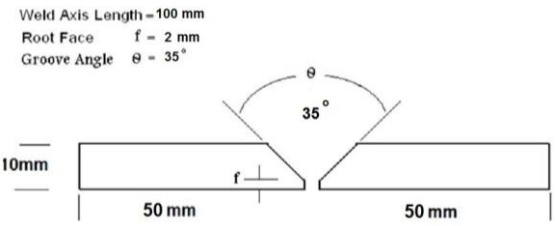

Fig. 1. Schematic illustration of of sample preparation with BS EN ISO 9692 standard and arrangement of welding specimens.

The microstructure of the prepared samples was examined using a light microscope SEM[1] (Meiji model) made in Japan with photography up to 1000x magnification. For this purpose, using sandpaper with ISO 6344 standard, P280, P400, P800, P1000, P1500, P2000 were sanded, respectively, and finally polished with felt and alumina suspension with a diameter of 1 micrometer to achieve a surface close to the mirror. After preparation, the samples were chemically

[1]Scanning Electron Microscope (SEM)

etched for 2 to 6 seconds using 2% nital solution (2% nitric acid and 96% ethanol alcohol) to reveal their microstructure.

Scanning electron microscopy (TEScan Vega model) was also used to examine the microstructure of the samples in more detail. The maximum resolution of this device is 3.5 nm with a magnification of 30,000 and its maximum operating voltage is 30 kV**.** Hardness test according to ISO 6506-1: 2014 standard was performed on the samples. This test was performed under ambient temperature. The diameter of the applied bullet was 10 mm, the applied force was N29420 and the application time was 20 seconds.

Tensile test specimens were prepared according to ASTM E 8 standard in the dimensions shown in Fig. 2**.** This test was performed based on ISO 6892-1: 2019 A23 and at ambient temperature with test speed and strain rate of 0.5-0.5 mm / mm / min. In order to evaluate the reproducibility of the results obtained from this test, three samples were analyzed and then the average of the results was reported.

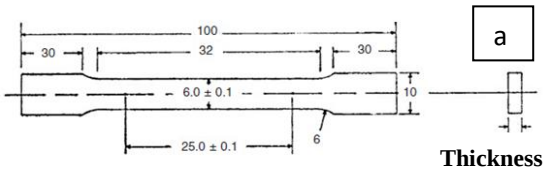

Fig. 2. a) Dimensions of the tensile test specimen according to ASTM E 8 standard (in millimeters).

Samples of this experiment were prepared according to ASTM E23-01 standard. This experiment was performed by Sharpe method Fig. 3.a and with a device belonging to Pars PEYGIR company, model PM29, at room temperature.

The dimensions of the impact sample according to the relevant standard are given in Fig. 3.b. In this analysis, the numbers reported were averaged from the results obtained from three samples in each case.

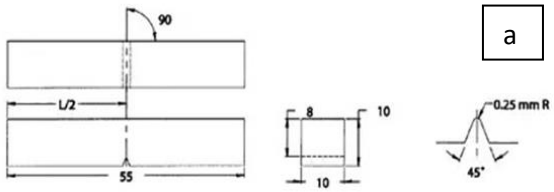

Fig. 3. a) Dimensions of Sharp impact sample (in millimeters).

3. Results and Discussion

3.1. Results of Microstructural Study

In order to observe the microstructure of base metals and compare it with the microstructure formed in the weld zone, the samples were examined at different magnifications by light and scanning electron microscopy. Fig. 4. shows light microscope images of the microstructure of St37 and 1.7225 (Mo40) base steels This steel contains 21% to 51% of grains. Fig. 4.a shows an optical microscope image of St37 steel**.**

Microscopic observations at various magnifications show that the phases in the microstructure of this steel include ferrite and needle ferrite grains along with areas and rows of perlite in the base metal St37.[19, 20, 21]. The phases are shown in Fig. 4.a Fig. 4.b shows the images made of 1.7225 (Mo40) alloy steel. According to the visible image, it can be concluded that the existing structure is mainly composed of bainite phase. Microscopic separation is also seen in some places**.**

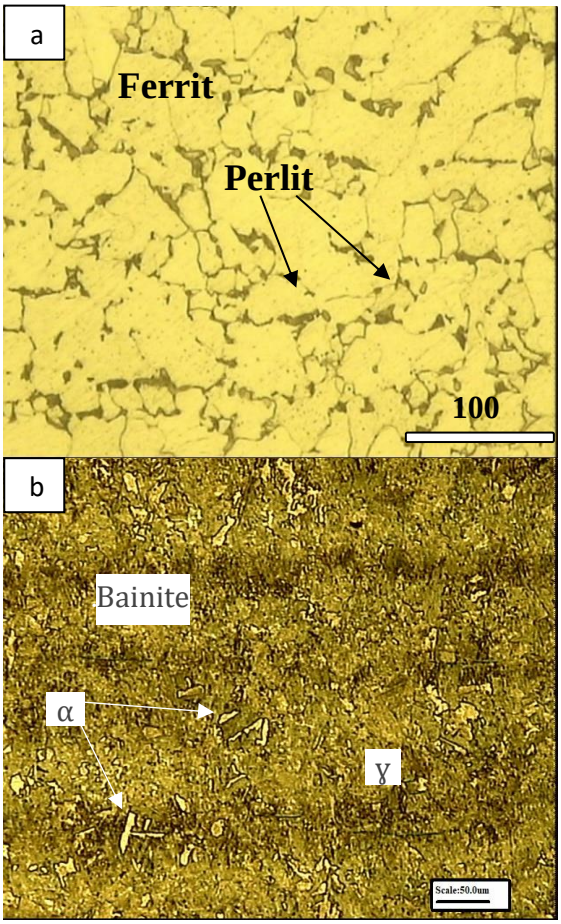

Fig. 4. a) Optical microscope images of St37steel, b) Optical microscope images of steel 1.7225 (Mo40).

Fig. 5. shows images taken using a scanning electron microscope made of 1.7225 (Mo40) and St37 steel. Fig. 5.a and Fig. 5.b show the images of the scanning electron microscope using the secondary electron detector at high magnification of 1.7225 (Mo40) and St37 steels, respectively. In

Fig. 5.b, the dark phase is the ferrite phase and the light phase is perlite. In this image, the nature of the perlite phase fingerprint is clearly known.

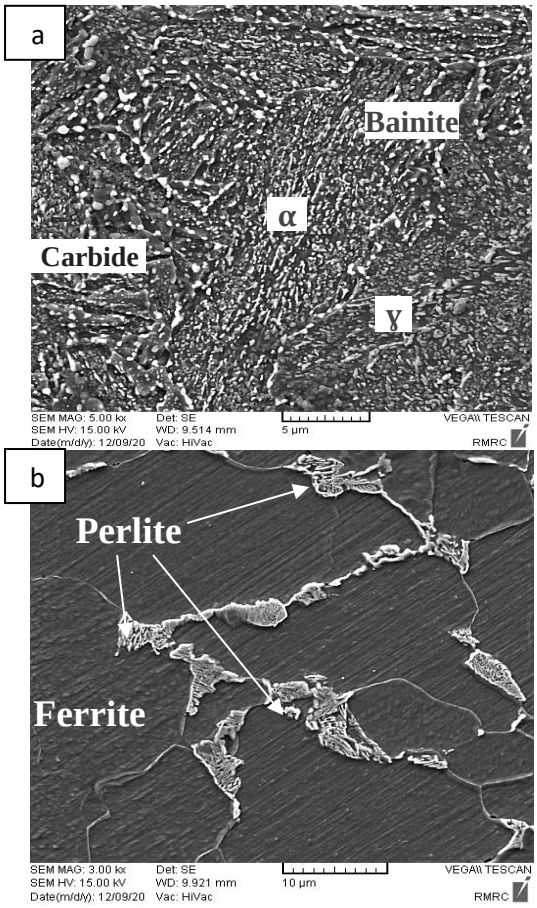

Fig. 5. SEM images obtained from a) 1.7225 (Mo40) steel at 5000x magnification and b) St 37steel at 3000x magnification.

Fig. 6. shows images obtained from light and SEM microscopes with secondary electron detectors at 100x and 1000x magnifications from the welded area and HAZ. Fig. 6.a shows an OM microscope image of the microstructure of the weld zone at the bottom and middle of the weld. According to the microstructural studies performed in connection with fuzzy morphology, it seems that the microstructure of the weld zone includes ferrite grains, needle ferrite and Wiedmann Statten with small amounts of perlite and cementite particles.

Research shows that primary Wiedmann-Staten ferrite germinates and grows directly from the surface of austenite grains, but secondary Wiedmann-Staton ferrite is derived from allotriomorphic ferrite present in the structure. Hence, the Wiedmann-Staten ferrite present in the structure is of a secondary type. Fig. 6.c also shows the SEM image of the microstructure of the weld zone at 1000x magnification. Fig. 6.d also shows the SEM image of the boundary between the welded and heat-affected areas. [21, 22, 23] Due to the fact that the microstructure of the HAZ region includes Wiedmann Staten ferrite and perlite, the difference between these two regions can be discerned in the image.

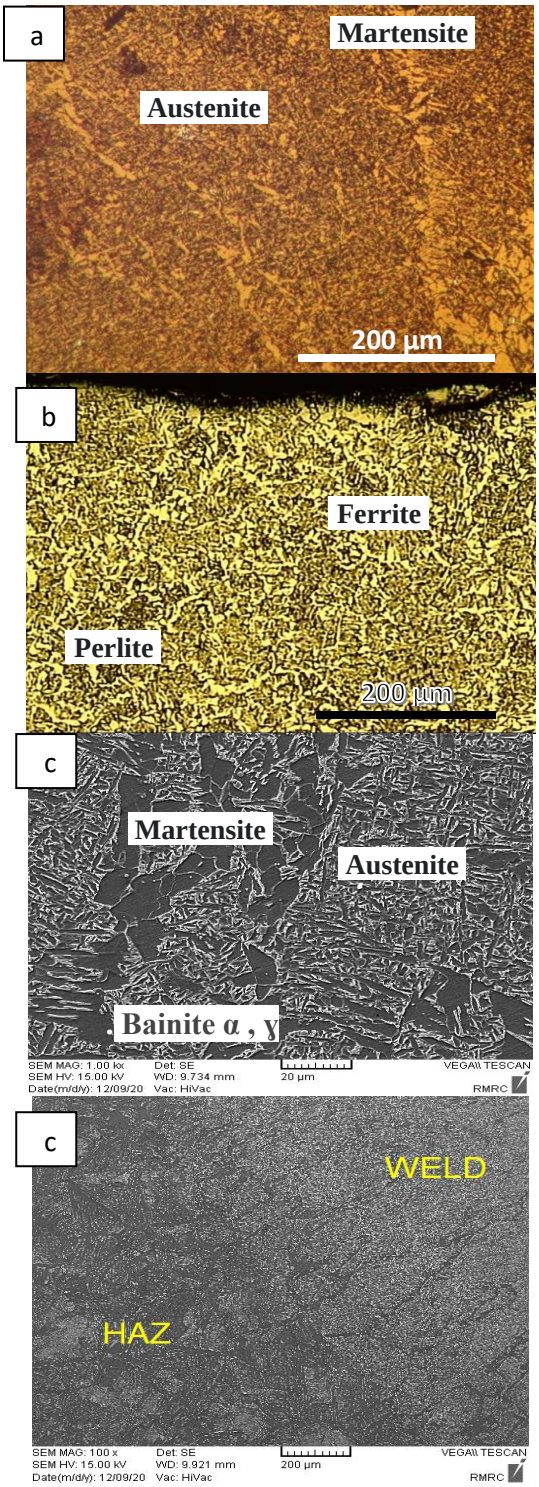

Fig. 6. Images from sample No. 1 using a light microscope. a) from the bottom and middle of the weld, b) from the top of the weld, images obtained using scanning electron microscopy c) from the weld zone and d) the joint and the HAZ area of St 37steel at 100x magnification.

Fig. 7. also shows images taken from samples 3 and 4 using OM and SEM microscopes.

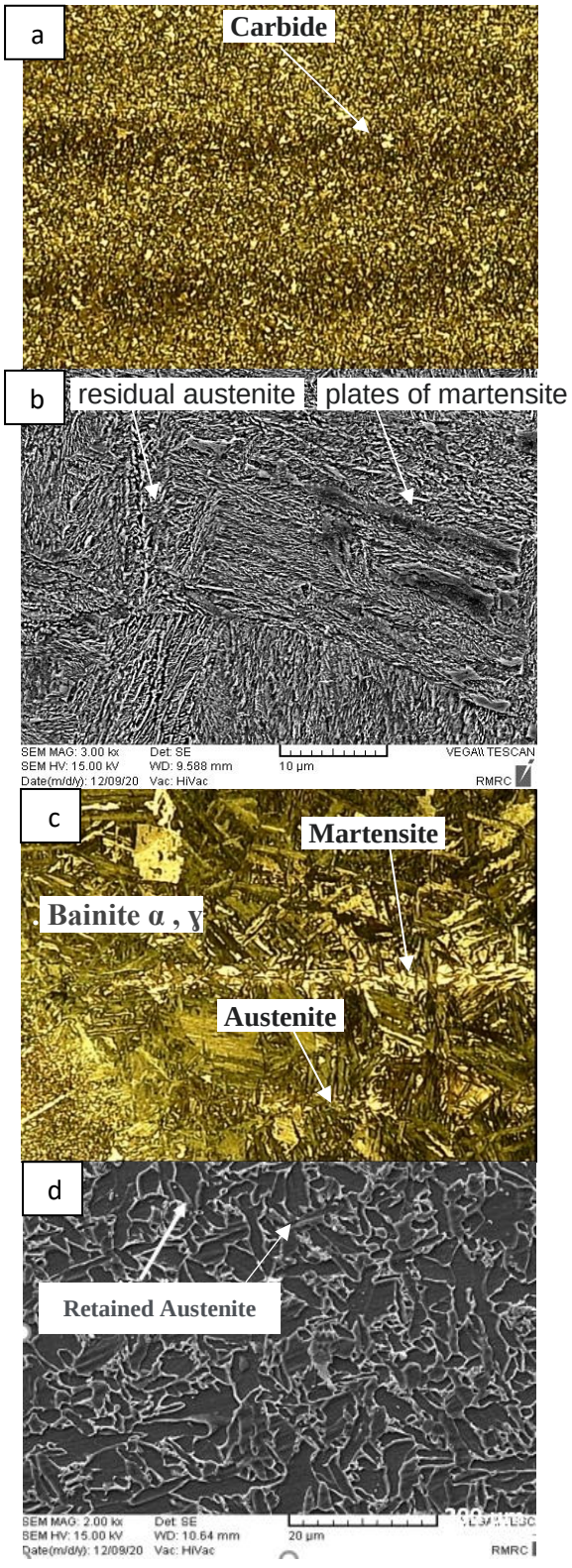

Fig. 7. a) OM image of sample No. 3of HAZ region 1.7225 (Mo40), b) SEM image of sample No. 3 of HAZ region side 1.7225 at 3000x magnification, c) OM image of sample No. 3 of HAZ region close to boiling and, d) SEM image of sample welding area No. 4at 2000x magnification.

The fine-grained structure is mainly visible in this area and microscopic separation effects are also observed in these areas.

Fig. 7.b shows the SEM Fig. 7.a shows the image of the HAZ microstructure on the side and adjacent to the base 72.1 alloy using a light microscope. image taken from Sample No. 3 of the same area at 3000x magnification. Fig. 7.c shows the image obtained using a light microscope from the HAZ area near and in the vicinity of the weld.

As shown in this image, residual austenite phase is observed at some points.

The reason for this phase can be attributed to the carbon content of the alloy of 1.7225. In general, the microstructure in this area includes martensite, coarse-grained bainite and some residual austenite.

Fig. 7.d also shows the SEM image obtained from the welding area of sample No. 4 at 2000x magnification.

Bainite occupies a region between these two process in a temperature range where iron self-diffusion is limited but there is insufficient driving force to form martensite.

The bainite, like martensite, grows without diffusion but some of the carbon then partitions into any residual austenite, or precipitates as cementite.

A further distinction is often made between so-called lower-bainite, which forms at temperatures closer to the martensite start temperature, and upper-bainite which forms at higher temperatures.

This distinction arises from the diffusion rates of carbon at the temperature at which the bainite is forming.

If the temperature is high then the carbon will diffuse rapidly away from the newly formed ferrite and form carbides in the carbon-enriched residual austenite between the ferritic plates leaving them carbide-free.

At low temperatures the carbon will diffuse more sluggishly and may precipitate before it can leave the bainitic ferrite. There is some controversy over the specifics of bainite's transformation mechanism; both theories are represented below.

3.2. Results of Mechanical Properties Tests

3.2.1. Tensile Test

Table. 4. shows the results of the tensile test performed on the samples. Among the reported values, samples No. 2 and No. 3 have the highest amount of tensile strength and yield and sample No. 9 has the lowest amount of tensile strength.

The final tensile strength of sample No. 3 with a preheating temperature of 250 °C and a duration of 20 minutes was 420 MPa and the yield strength was 284 MPa. Sample No. 2 with tensile and yield strength, 412 MPa and 276 MPa also has the highest amount of strength among the samples after Sample No. 3.

Table. 4. Results of tensile test for different samples.

Percentage of Relative Elongation (%)	Yield Strength (MPa)	Ultimate Tensile Strength (MPa)	Sample
15	252	390	**1**
22	276	412	**2**
27	284	420	**3**
21/5	268	403	**4**
22	252	384	**5**
13	241	379	**6**
23	240	372	**7**
13	254	361	**8**
11	258	359	**9**
21	259	393	**10**
25	270	410	**11**
27	235	370	**12**

Due to the fact that sample No. 3 has been heated for a longer period of time than samples No. 1 and No. 2, it is expected that the temperature distribution on the surface and core of this part will be the same. Due to the **Hall-Patch** [23, 24, 25] relationship and because sample number 3 has been in the preheating temperature of 250 °C for a longer period of time than samples No. 1 and No. 2, it is expected that the temperature distribution will be almost the same everywhere. This will reduce the defects in the joint area and therefore will increase the strength of the sample. Sample No. 1 has the lowest strength compared to Samples No. 2 and No. 3, and this is due to its less preheating time.

Based on microscopic examinations performed using a light microscope, it was determined that there was a defective melting defect or lack of fusion in the welding structure of this sample, and in one part of the weld, no connection was established with the base metal [26]. Fig. 9. shows the image of the non-fusion area. This will greatly affect the final tensile strength and yield of this specimen.

According to Table. 4., and Fig. 8. the final tensile strength of specimens 4 to 6 preheated to 350 °C is 403 MPa, 384 MPa and 379 MPa, respectively. By comparing the amount of tensile strength of sample No. 4(preheating temperature 350 °C and duration 10minutes) with samples No. 2 and No. 1, it can be seen that there was almost a slight difference between them, in the sound that the percentage of relative elongation of the sample Number 4 is the same as sample number 3, which showed the best result. Unlike samples 1 to 3, which had a minimum preheating temperature of 250 °C, with increasing the preheating time to 350 °C, the tensile strength and yield of the samples decreased.

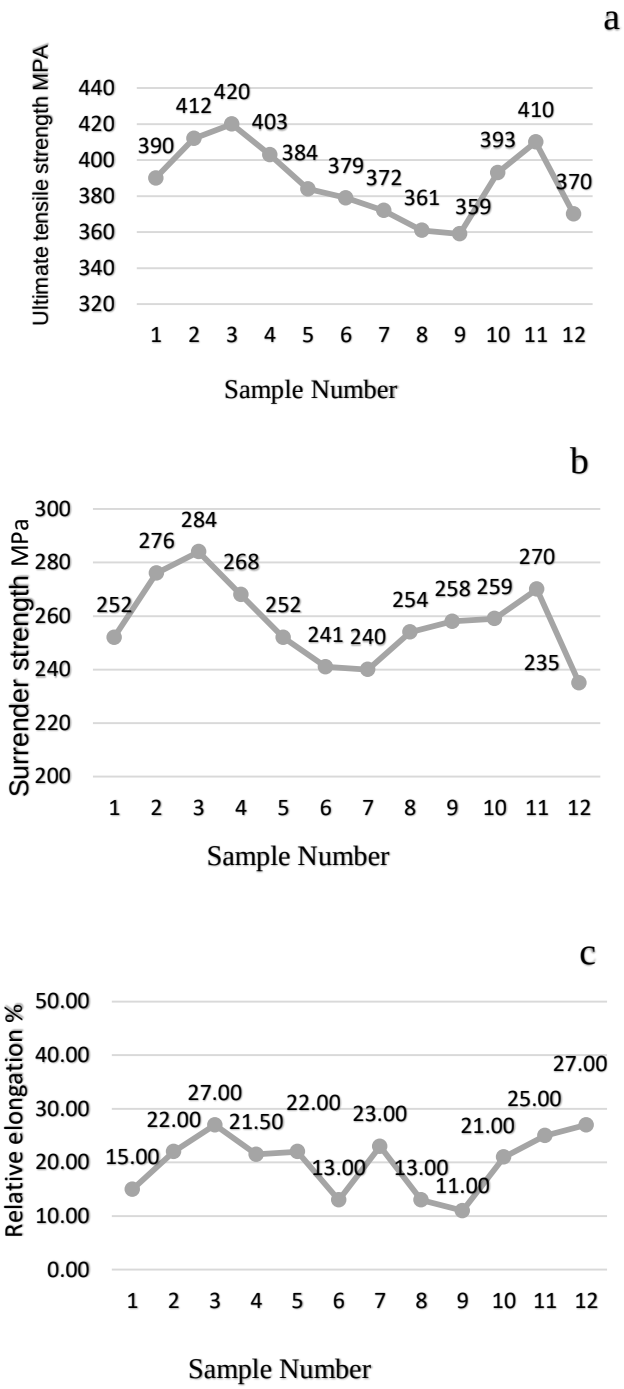

Fig. 8. a. Graph of changes related to independent final tensile strength in MPa, b. Surveillance strength diagram in MPa, c. The percentage of relative elongation is related to the samples studied in this study.

Among samples 4 to 6, sample 4has the highest strength and sample number 6 has the lowest value. In the case of samples 7 to 9 (which are preheated at 450 °C), it can be seen that the sample with the shortest preheating time has the highest tensile strength in this temperature range.

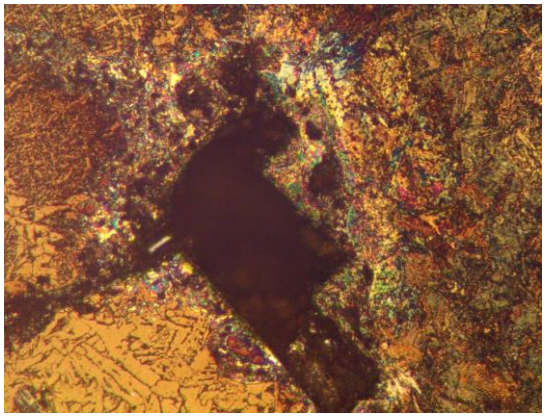

Fig. 9. Image of the area with the defect of non-fusion and separation in sample No. 1.

According to the obtained results, the effect of preheating temperature and its duration on welded samples can be observed to some extent [27]. In the case of welded specimens with preheating temperatures of 350 °C and 450 °C, it was observed that the shorter the preheating time, the higher the final tensile strength of the part.
This is because by reducing the preheating time, the preheating process of the sample and reaching the set temperature on the surface and the brain is not done properly and this prevents the grains from coagulating. Since the grain size in the joint area of two steels is one of the most important factors determining the strength of the part, as a result, the strength of the sample to the tensile stress applied to it increases with decreasing preheating time. On the other hand, by changing the cooling rate in the samples, the resulting microstructures along with the grain size have changed and therefore the values related to the final tensile strength, yield and failure will be different [28].
In samples No. 7, No. 8 and No. 9, the volume fraction of the ferrite phase has increased and therefore the mechanical properties of these samples have significantly decreased compared to the samples No. 3 and No. 2 with microstructure including Weidman Staten ferrite and martensite. In the case of samples No. 10 to No. 12, which have been subjected to the welding process by the TIG welding method, it is also observed that the tensile strength and yield are relatively high. In general, in the samples studied in this project, with increasing the preheating temperature, the cooling rate decreases due to the same temperature and preheating time of these samples with 4 to 6 samples (which are welded by CO_2 method). It is observed that the tensile strength and yield of samples 10 to 12 in the Tig method are higher than samples 4 to 6 in the CO_2 method.
Of course, this difference is not significant, but as a result, the high quality of the connection is achieved. This causes an increase in grain size and further recrystallization in the HAZ area, with increasing preheating temperature more sediments accumulate in the boundaries and slip bands.
Accumulation of sediments in the grain boundaries has caused the scattered sediments to accumulate in a continuous network in the grain boundaries and the ground is emptied of this hard phase. Emptying the ground from this hard phase and increasing the grain size by reducing the cooling rate can affect the strength to some extent [29].

3.3. Impact Test Results

Table. 5. and Fig. 10. and Fig. 11. show the results of the impact test for the samples. The maximum and minimum values obtained in this experiment are for samples 9 and samples 1, respectively.
The reason for this is that the sample number 9 has a higher preheating temperature than the other sample and as a result has more inlet heat, which will be longer for it to cool down.
Due to the slowing down of cooling, the seeds take longer to grow and as a result, the final microstructure will be larger.
It should be noted that grain size has a significant effect on impact fracture toughness. According to studies, with increasing grain size, impact fracture toughness increases [30].

Table. 5. Impact test results for different samples tested (Joule).

Impact Energy (J)	Sample Number (Quantity)
36	**1**
42	**2**
46	**3**
51	**4**
60	**5**
66	**6**
66	**7**
68	**8**
70	**9**
43	**10**
44	**11**
46	**12**

Fig. 11. presents the results of the hardness test. Hardness test was performed on the welding area of the samples and at certain distances from it. As can be seen in Table. 5., the highest hardness value is obtained for sample number 1 and the lowest hardness value is reported for sample number 9.
The preheating time and temperature of samples 1 and sample 9 are 10 minutes, 250 °C and 20 minutes and 450 °C, respectively.
According to the phases formed in the microstructure of the weld zone and its adjacent areas and also the comparison of these areas with each other, the obtained results can be examined. By comparing the hardness numbers obtained from

samples 1 to samples 3 (which were obtained equal to 246 Vickers, 239 Vickers and 237 Vickers, respectively), Fig. 10. a decreasing trend in the hardness of the weld zone can be observed. This may be due to the shorter exposure time of sample 1 compared to sample 2 and sample 3 at a preheating temperature of 250 °C. Examples 4 to 6, like Examples 7 to 9, show this decreasing trend.

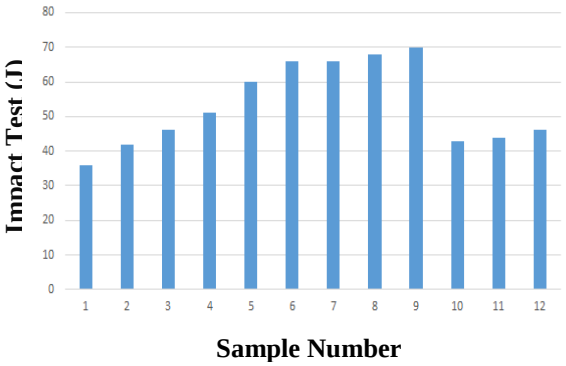

Fig. 10. Column diagram of impact Test changes for different samples.

This can be attributed to the fact that by increasing the sample period of the sample at a certain temperature, its cooling rate tends to decrease as well as the high temperatures of the baseline, and the percentage of soft phase like Frith also increases. In Fig. 11., the stiffness profile from the weld zone to the baseline steels St37 and 1.7225 (Mo40) is provided with 3 samples to No. 1, No. 4, and No. 9. Given the chemical composition of alloy steel 1.7225 (Mo40) and low alloy Carbon steels St37, the difference of hard numbers on both sides of the natural binding site is normal.

By distancing themselves from the weld zone to the alloy steel of 1.7225 (Mo40), the stiffness number increases relative, while the trend is sharply reduced to the steel of St37 , and then the procedure is first increased and then stabilized.

Due to the research done and the difficult observable difference from the baseline steels , the weld zone is expected to have less hardness than steel with high hardness and higher hardness compared to steel [31, 32, 33, 34].

As shown in Fig. 11., the hard number obtained in the weld zone lies in the range between the hard numbers of the baseline steels. in general, the changes in the hardness of parts can be due to changes in the size of the seeds and the formation of hard deposits in the microstructure or microstructure of the microstructure. accuracy is observed in the process of hard numbers on the side of alloy 1.7225 (Mo40), which has a hard number in most cases within 1 Cm distance of the weld zone. in contrast to this trend , St37 by distance from joining site , St37 is caused by a sharp drop in stiffness which increases with increasing this distance [33, 34].

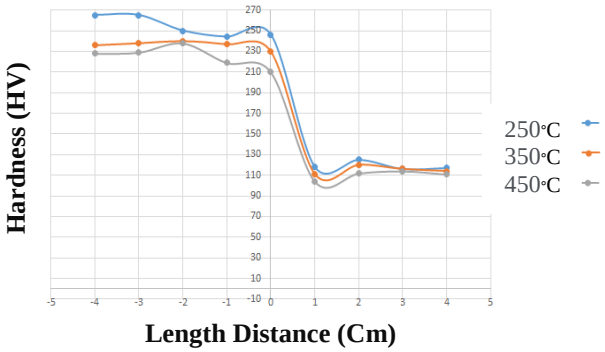

Fig. 11. Hardness profile from the welding site to the base steels on the sides of samples 1, 4 and 9.

The comparison of the hardness profiles at different temperatures indicates that the results of this study show that the high temperature of the alloy is very high. Due to the high temperature of the alloy at low temperatures, the sediments are depleted and these sediments are formed.

4. Conclusion

According to the tests and studies performed, the results are as follows :

1. Microstructural studies showed that the microstructure of the weld zone of the specimens included ferrite, Wiedman-Staten ferrite, along with small amounts of fine cementite, perlite and Martensite particles. The microstructure of St 37 steel is ferrite-perlite and the phases in 1.7225 (Mo40) alloy steel are mainly Bainite.
2. The temperature variation of samples from 250 °C to 450 °C has resulted in a change in the cooling rate of samples in the joint and their HAZ regions, which resulted in variations of phase and grading in the weld zone microstructure.
3. by increasing the temperature, the sample cooling rate increased, followed by increasing the grain size and the volume fraction of soft phases such as Frith.
4. The results showed that specimen 3 with tensile strength and yield stress yield 420 MPa and 284 MPa, respectively, with Tensile strength and tensile strength Mpa, 359 Mpa and 258 Mpa, respectively.
5. In the impact test data, it was observed that sample number 9 with 70 joules has the highest failure rate among the samples, which is due to the high duration and preheating temperature of this sample. On the other hand, the fracture toughness of sample number 1 was calculated as the lowest value and equal to 36 joules, which was welded in the shortest time and preheating temperature.
6. In the hardness test, the numbers obtained from the test show that the highest hardness number with a value of 250 HV is related to sample 10 and the lowest is related to sample 9 with a value of 210 HV. 7. Also, based on the profiles extracted from the welding area and adjacent areas, it was

determined that the hardness number of the joint area is between the values of 1.7225 (Mo40) and St37 steels.

References

[1] L. Jeffus, “Welding: Principles and Applications”, Cengage Learning., 2016.
[2] M. A. Reeser, Cool Springs Press., 2017.
[3] H. Sabet, "Welding technology and metallurgy", 2008.
[4] R. S. Mishra, P. Sarathi De and N. Kumar, Technol. Eng., Springer, 2014.
[5] H. Sabet and N. Mirza Mohammad, "Welding Technology and Metallurgy", 2008.
[6] H. Saatchi, H. Idris, "Steel Key", Arkan Danesh, 2001.
[7] K. Li, F. Jarrar, J. Sheikh-Ahmad amd F. Ozturk “Welding Process and Its Parameters - Friction Stir Welding”, 207, 2017, 574.
[8] J. Vora and V. J. Badheka, “Advances in Welding Technologies for Process Development”, CRC Press., 2019.
[9] M. Azizieh, M. Khamisi, Int. J. Adv. Manuf. Technol., 2016, 2773.
[10] E. El-Kashif and M. A. Morsy, IIW 2017 Int. Conf., At: Shanghai China, June, 2017.
[11] B. P. Srivastava, S. P. Tewari and J. Prakash, “A Rev. Int. J. Eng. Sci. Technol., Vol. 2 (4), 2010, 625.
[12] Teng, Tso-Liang, Chang, Peng-Hsiang, "A Study of Residual Stresses in Multi-Pass Girth-Butt Welded Pipes", Int. J. of Pressure Vessels and Piping, 74, (1997), 59.
[13] S. Lee, B. C. Kim and D. Kwon, Metall. Trans., A, 1992.
[14] Q. Xue, D. Benson, M. A. Meyers, V. F. Nesterenko and E. A. Olevsky, Mater. Sci. Eng. A354, (2003), 166.
[15] E. Ramirez, S. Mishael and R. Shockley, Welding Res., Welding J., (2005).
[16] S. Jinlong and Q. Xiaoming, Licensee MDPI, Basel, Switzerland, 2019.
[17] A. G. Olabi and G. Casalino, Comp. Mater. Process., Vol. 6, 2014, 101.
[18] N. Khodabandehlo and H. Sabet, , 2015. https://civilica.com/doc/1024378
[19] S. R. Amirabdizade, S. Shafinia, H. Sabet, S. Mirdamadi and H. Ebrahimnezhad-Khaljiri, Metallography Microstructure LLC and Analysis part of Springer Nat. and ASM Int., 2018, 1.
[20] I. Hajiannia, M. Shamaniyan, M. R. PakManesh and M. Kasiri, Mater. Eng., 2021, Volume 2 (Consecutive Number 45), 1397, 1.
[21] H. Sabet, M. R. Farzin, B. Abedini and M. M. Hosseinion, , 10th National Conf. on Welding and Insp., Tehran, 2009.https://civilica.com/doc/859527
[22] M. Ramezani Movafaq, M. Naderi, M. A. Soltani and R. Baradaran, J. Metall. Eng., Volume 17, 54, 53 Summer 2014, 18.
[23] W. D. Callister, Fundamentals of Mater. Sci. Eng., 2nd ed. Wiley & Sons., 252.
[24] F. Smith, F. William and J. Hashemi, Found. Mater. Sci. Eng. (4th ed.), McGraw-Hill, 2006.
[25] G. E. Dieter, Mech. Metall., Third Edition, McGraw-Hill, 2017.
[26] M. R. Taheri, H. Sabet and B. Karbakhsh, 18th National Conference on Welding and Insp. and 7th Natl. Conf. on Non-Destructive Testing, Arak, 1396. https: / /civilica.com/doc/731316.
[27] A. Talebi, R. Bakhtiari and B. Abbasi Khazaei, J. Metall. Eng., 17, 53, Spring 2014, 40.
[28] R. Saberi, E. H. Dehkordi and A. Khodabandeh, Jihad Daneshgahi Scientific Information Center, 2010.
[29] S. Salimifar, D. Davoodi, S. Salahshor, A. Lotfi, Quarterly J. Adv. Mater. Technol., 4, 2, Summer 2015, 53.
[30] Li, Wen-Lan., C. M. J. Li., Philos. Mag. A, Vol. 59, 2006.
[31] Tadashi Kasuya, Nobutaka Yurioka, Makoto Okumura, Nippon Steel Tech. Rep. No.65, (1995).
[32] B. Eigenmann, V. Schulze and O. Vo¨hringer, Society of Experimental Mechanics, Bethel, Connecticut, Baltimore, MD, 1994, 598.
[33] Y. C. Lin and K. H. Lee, J. Mater. Process. Technol., 63, 1997, 797.
[34] J. Qamaruzzaman, M. Mazni, M. H. Ismail, A. Muchtar, M. Selamat and R. Ahmad, Mater. Sci. Eng., 834, 2020, 12.